Cent. Eur. J. Phys. • 6(3) • 2008 • 479-490
DOI: 10.2478/s11534-008-0067-4

VERSITA

Central European Journal of **Physics**

Temperature and electric field dependences of the mobility of electrons in vertical transport in GaAs/$Ga_{1-y}Al_yAs$ barrier structures containing quantum wells

Research Article

Safi Altunöz[12], Hüseyin Çelik[1], Mehmet Cankurtaran[1]*

1 Hacettepe University, Faculty of Engineering, Department of Physics, Beytepe, 06800 Ankara, Turkey

2 Present address: Ministry of Environment and Forestry, General Directorate of State Hydraulic Works, Department of Technology, Yücetepe, 06100 Ankara, Turkey

Received 4 January 2008; accepted 27 February 2008

Abstract: The mobility of electrons in vertical transport in GaAs/$Ga_{1-y}Al_yAs$ barrier structures was investigated using geometric magnetoresistance measurements in the dark. The samples studied had $Ga_{1-y}Al_yAs$ ($0 \leq y \leq 0.26$) linearly graded barriers between the n^+-GaAs contacts and the $Ga_{0.74}Al_{0.26}As$ central barrier, which contain N_w (=0, 2, 4, 7 and 10) n-doped GaAs quantum wells. The mobility was determined as functions of (i) temperature (80-290 K) at low applied voltage (0.01-0.1 V) and (ii) applied voltage (0.005-1.6 V) at selected temperatures in the range 3.5-290 K. The experimental results for the temperature dependence of low-field mobility suggest that space-charge scattering is dominant in the samples with N_w=0 and 2, whereas ionized impurity scattering is dominant in the samples with N_w=4, 7 and 10. The effect of polar optical phonon scattering on the mobility becomes significant in all barrier structures at temperatures above about 200 K. The difference between the measured mobility and the calculated total mobility in the samples with N_w=4, 7 and 10, observed above 200 K, is attributed to the reflection of electrons from well-barrier interfaces in the quantum wells and interface roughness scattering. The rapid decrease of mobility with applied voltage at high voltages is explained by intervalley scattering of hot electrons.

PACS (2008): 72.20.Fr, 72.20.Dp, 73.43.Qt, 73.40.Ty

Keywords: barrier structures • vertical transport • geometric magnetoresistance • mobility • hot electrons • scattering mechanisms • drift velocity

© *Versita Warsaw and Springer-Verlag Berlin Heidelberg.*

1. Introduction

Investigation of vertical transport of electrons and scattering mechanisms in barrier structures containing quantum wells is of great importance in understanding the physical properties of various advanced electronic devices, such

*E-mail: cankur@hacettepe.edu.tr

Brought to you by | Hacettepe Ueniversitesi
Authenticated
Download Date | 3/12/20 1:58 PM

as quantum-well infrared photo-detectors (QWIPs), heterostructure bipolar transistors, semiconductor lasers, and hot-electron transistors (for a review see [1]). For instance, the vertical transport of electrons has a direct influence on the performance of QWIPs. Various scattering processes affect the electron mobility along the growth direction, influencing the well-capture probability, a parameter that is directly related to the detector's optical gain and responsivity.

Barrier structures with rectangular potential barriers have been studied extensively (see [1]). Recently, Ridley and coworkers [2–6] investigated vertical transport in GaAs/$Ga_{1-y}Al_yAs$ barrier structures with linearly graded barriers grown between the n^+-GaAs contacts and the central barrier containing N_w (=0, 2, 4, 7 and 10) quantum wells. Bishop *et al.* [4] measured the electron mobility as a function of temperature in the range 77–300 K by applying low voltage (0.01 V) to the samples with N_w =4, 7 and 10. They did not, however, measure the variation of electron mobility with applied voltage. Daniels *et al.* [5] proposed a theoretical model to account for the effect of the quantum wells in the central barrier on the electron mobility. Nevertheless, the scattering mechanisms that determine the temperature and applied voltage dependences of the electron mobility in these barrier structures have not been investigated in detail.

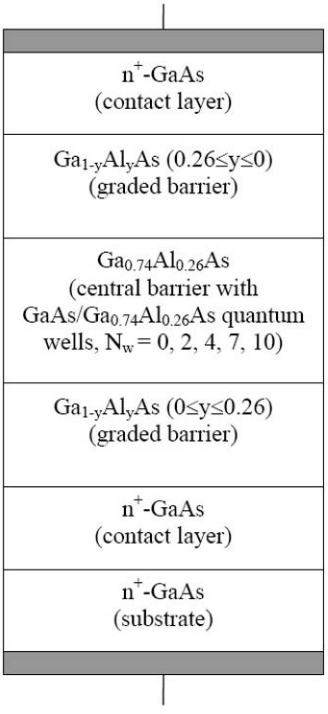

Figure 1. The layer structure of the samples used in the study.

In this paper we present a systematic study of the effects of temperature and applied voltage on the mobility of electrons in vertical transport in barrier-structure samples, which were prepared from the same wafers as those used in [4]. The electron mobility was determined from geometric magnetoresistance (GMR) measurements carried out in the dark. The scattering processes affecting the electron mobility were analysed as functions of temperature and applied voltage. The present study provides valuable information about the relative importance of various scattering mechanisms that limit the mobility of electrons in these barrier structures.

2. Theoretical background

The major scattering mechanisms in GaAs/$Ga_{1-y}Al_yAs$ barrier structures without quantum wells are essentially the same as those in bulk $Ga_{1-y}Al_yAs$ alloys. These mechanisms include ionized impurity scattering, space-charge scattering, alloy-disorder scattering, polar optical phonon scattering, acoustic phonon scattering due to the deformation potential coupling, and acoustic phonon scattering due to the piezoelectric coupling [7, 8]. However, additional scattering processes, such as quantum-mechanical reflection due to well-barrier interfaces [5, 9] and interface roughness (IFR) scattering, play a role in limiting the electron mobility in the barrier-structure samples containing quantum wells. The total mobility (μ_{tot}) can be calculated from the individual scattering-limited mobilities (μ_i) by using Matthiessen's rule:

$$\frac{1}{\mu_{tot}} = \sum_i \frac{1}{\mu_i} = \sum_i \frac{e\tau_i}{m^*}, \tag{1}$$

where e is the magnitude of the electron charge, τ_i is the momentum relaxation time, and m^* is the electron effective mass. In the following, the approximate analytical expressions that we used to calculate the electron mobility (μ_i) determined by each scattering mechanism are briefly outlined for the sake of convenience.

2.1. Ionized impurity scattering

Ionized impurity scattering is an important mechanism, which limits the electron mobility in semiconductors. The mobility (in units of $m^2V^{-1}s^{-1}$) determined by ionized impurity scattering (μ_{ii}) can be obtained from [8, 10]

$$\mu_{ii} = \frac{128(2\pi)^{1/2}(k_B T)^{3/2}(\varepsilon_s\varepsilon_0)^2 e^{-3}(m^*)^{-1/2}(2N_i)^{-1}}{\left[\ln(1+n_0) + \dfrac{n_0}{1+n_0}\right]} \tag{2}$$

Brought to you by | Hacettepe Ueniversitesi
Authenticated
Download Date | 3/12/20 1:58 PM

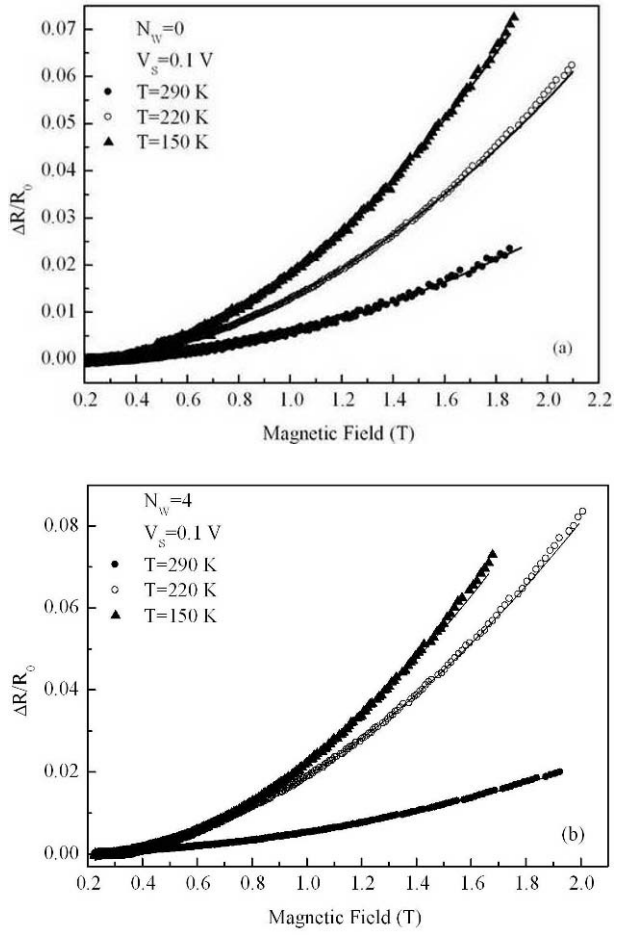

Figure 2. The variation of fractional magnetoresistance ($\Delta R/R_0$) with magnetic field for the samples with (a) N_w=0 and (b) N_w=4 measured at an applied voltage V_S=0.1 V and at different temperatures (T) as quoted. The symbols correspond to the experimental data, and the full curve through each set of data points represents the parabola (Eq. (12)) that best fits the experimental data.

where

$$n_0 = \frac{6\, k_B\, T\, m^*}{\pi^{3/2}\hbar^2\, |N_D - N_A|^{2/3}}. \tag{3}$$

Here k_B is the Boltzmann constant, T is the absolute temperature, ε_s is the static dielectric constant, ε_0 is the permittivity of vacuum, $\hbar$ is the Planck constant, N_i is the ionized impurity density, and N_D and N_A are the ionized donor and acceptor impurity densities, respectively. (For p-type and n-type doped materials, N_i can be taken equal to N_A and N_D, respectively). Several experimental studies published in the literature show that ionized impurity scattering is effective in bulk $Ga_{1-y}Al_yAs$ alloys at low temperature [7, 11–14].

2.2. Acoustic phonon scattering

The mobility (μ_{DP}) determined by acoustic deformation potential scattering can be calculated using

$$\mu_{DP} = \frac{2^{3/2}\pi^{1/2}\hbar^4 e C_L}{3E_A^2 (m^*)^{5/2}(k_B T)^{3/2}}. \tag{4}$$

Here C_L is the longitudinal elastic stiffness constant (see Eq. (6)) and E_A is the acoustic deformation potential [7, 8].

Because of the lack of inversion symmetry in $Ga_{1-y}Al_yAs$ crystals, there is another source of scattering due to piezoelectrically active acoustic phonons. The mobility (μ_{PE}) limited by the acoustic piezoelectric scattering can be obtained from [8]

$$\mu_{PE} = \frac{16(2\pi)^{1/2}\hbar^2\varepsilon_s\varepsilon_0}{3eK_{av}^2 (m^*)^{3/2}(k_B T)^{1/2}} \tag{5}$$

with

$$K_{av}^2 = \frac{e_{14}^2}{\varepsilon_s\varepsilon_0}\left(\frac{12}{35C_L} + \frac{16}{35C_T}\right). \tag{6}$$

Here K_{av}^2 is the average electromechanical coupling constant, e_{14} is the piezoelectric stress constant, and C_L and C_T are the spherical-average, longitudinal and transverse elastic stiffness constants of a single-crystal with cubic symmetry, respectively [7, 15]. Earlier studies indicate that acoustic phonon scattering is not significant in the determination of electron mobility in bulk $Ga_{1-y}Al_yAs$ [7, 11–14].

2.3. Polar optical phonon scattering

Because of the high values of the optical phonon energy, optical phonon scattering in semiconductors is an inelastic process, and a momentum relaxation time cannot be defined for polar optical phonon scattering. Nevertheless, the following expression [16] can be used as an approximation to estimate the mobility (μ_{PO}) due to polar optical phonon scattering:

$$\mu_{PO} = \frac{16\hbar^2\varepsilon_0\,(2\pi k_B T)^{1/2}}{3e(\,m^*)^{3/2}\left(\frac{1}{\varepsilon_\infty} - \frac{1}{\varepsilon_s}\right)} \frac{1}{\left(\frac{k_B T_{PO}}{e^{\frac{T_{PO}}{T}} - 1}\right)} \chi\left(\frac{T_{PO}}{T}\right). \tag{7}$$

Here ε_∞ is the high-frequency dielectric constant, $T_{PO}(=\hbar\omega_{PO}/k_B)$ is the longitudinal optical-phonon temperature, and $\chi(T_{PO}/T)$ is an integral function. For $Ga_{1-y}Al_yAs$

Brought to you by | Hacettepe Ueniversitesi
Authenticated
Download Date | 3/12/20 1:58 PM

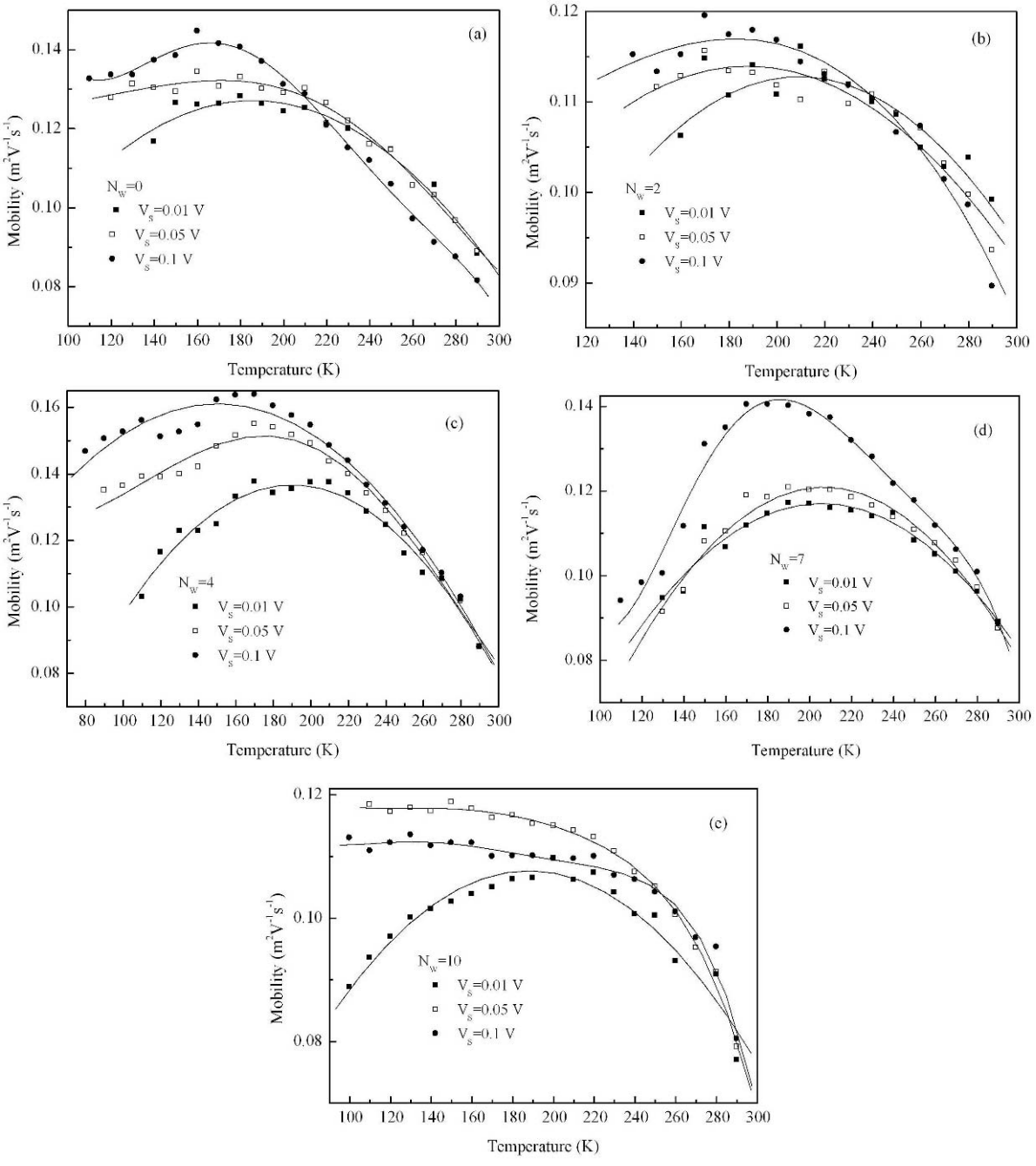

Figure 3. Temperature dependence of the electron mobility for the barrier-structure samples containing (a) N_w=0, (b) 2, (c) 4, (d) 7 and (e) 10 quantum wells, measured at different applied voltages (V_S) as quoted. The symbols represent the experimental data, and the full curves through the experimental data points are intended to be a guide to the eye.

alloys, Look [8] obtained the following expression for $\chi(T_{PO}/T)$, which is valid at high temperatures ($T > 84$ K):

$$\chi\left(\frac{T_{PO}}{T}\right) = 1 - 0.5841\left(\frac{T_{PO}}{T}\right) + 0.2920\left(\frac{T_{PO}}{T}\right)^2 - 0.037164\left(\frac{T_{PO}}{T}\right)^3 + 0.0012016\left(\frac{T_{PO}}{T}\right)^4. \quad (8)$$

Brought to you by | Hacettepe Ueniversitesi
Authenticated
Download Date | 3/12/20 1:58 PM

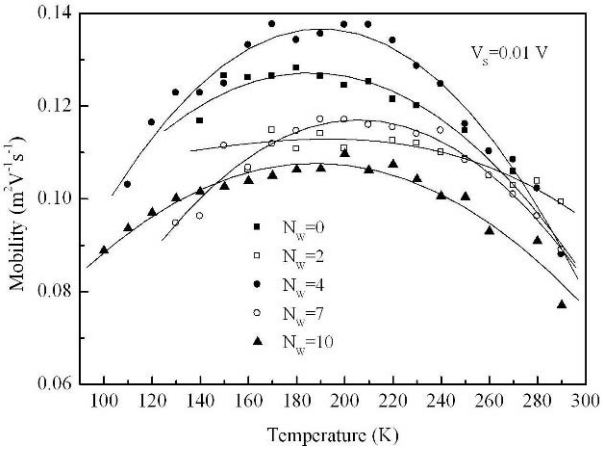

Figure 4. Comparison of the mobility-temperature curves measured at low applied voltage (0.01 V) for the barrier-structure samples containing N_w quantum wells. The symbols represent the experimental data, and the full curves through the experimental data points are intended to be a guide to the eye.

The scattering of electrons by optical phonons through the deformation potential interaction is not important for the Γ valley of the conduction band in $Ga_{1-y}Al_yAs$ alloys [7, 8] and is thus not considered in the present study.

2.4. Space-charge scattering

The mobility (μ_{SC}) determined by space-charge scattering can be calculated using

$$\mu_{SC} = \frac{e}{(2m^* k_B T)^{1/2} N_S A}, \tag{9}$$

where N_S is the space-charge density and A is the effective scattering area of the space-charge region [17]. Previous studies [7, 11–13, 18, 19] show that, in bulk $Ga_{1-y}Al_yAs$ alloys, space-charge scattering becomes effective at higher temperatures than ionized impurity scattering.

2.5. Alloy-disorder scattering

The relaxation time due to alloy-disorder scattering was determined by Hauser *et al.* [20]. The temperature dependence of the mobility (μ_A) limited by alloy-disorder scattering can be expressed as [7, 13]

$$\mu_A = \frac{2^7 (2)^{1/2} e\hbar^4}{9\pi^{3/2} a^3 (m^*)^{5/2} y(1-y)(\Delta U)^2 (k_B T)^{1/2}}, \tag{10}$$

where a is the lattice constant, y is the Al molar fraction, and ΔU is the alloy-disorder potential of $Ga_{1-y}Al_yAs$.

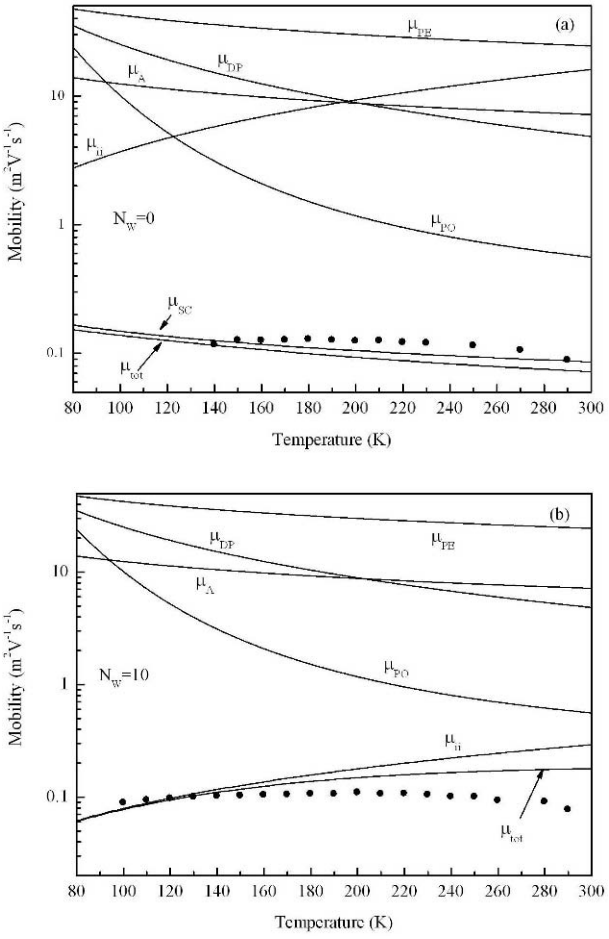

Figure 5. Temperature dependence of the electron mobility measured at 0.01 V (full circles) for the barrier-structure samples containing (a) N_w=0 and (b) N_w=10 quantum wells and the calculated mobilities (full curves). μ_A, μ_{DP}, μ_{PE}, μ_{PO}, μ_{ii} and μ_{SC} are the mobilities determined by alloy disorder, acoustic deformation potential, acoustic piezoelectric, polar optical phonon, ionized impurity and space-charge scattering, respectively, and μ_{tot} is the calculated total mobility.

The mobilities limited by alloy-disorder and space-charge scattering mechanisms have identical temperature dependence. However, it has been shown that alloy-disorder scattering does not play an important role in the determination of electron mobility in $Ga_{1-y}Al_yAs$ (y <0.32) alloys [7, 8, 13, 19].

2.6. Intervalley scattering

Because of the small dimensions of the barrier-structure samples, the electric field within the structure becomes very high, even at low applied voltages. When the applied voltage is increased, the conduction electrons gain kinetic

Brought to you by | Hacettepe Ueniversitesi
Authenticated
Download Date | 3/12/20 1:58 PM

Table 1. Structural properties of the barrier-structure samples used in the study.

Sample	Number of quantum wells N_w	Width of the barrier layer between the quantum wells L_B [Å]	Quantum well width L_W [Å]	Total thickness of barrier layers L [Å]	Doping density in contact layer [10^{23} m^{-3}]
QT680A	0	-	-	2084	8
QT680E	2	1006	35	2076	9.5
QT680D	4	310	35	2070	9
QT680C	7	135	35	2055	7
QT680B	10	77	35	2043	8

energy from the electric field, and their energy becomes higher than the thermal equilibrium value $3k_BT/2$. The electrons, which are not in thermal equilibrium with the crystal lattice, are known as hot electrons (see for instance [21]). As the applied electric field becomes higher than a critical value, hot electrons scatter from the Γ valley into the L (and X) valleys. Within the framework of a three-valley, conduction band model, the Hall mobility (μ_H) is given by [11, 13, 18]

$$\mu_H = \mu_\Gamma \frac{\left[1 + \frac{n_X}{n_\Gamma}\left(\frac{\mu_X}{\mu_\Gamma}\right)^2 + \frac{n_L}{n_\Gamma}\left(\frac{\mu_L}{\mu_\Gamma}\right)^2\right]}{\left(1 + \frac{n_X}{n_\Gamma}\frac{\mu_X}{\mu_\Gamma} + \frac{n_L}{n_\Gamma}\frac{\mu_L}{\mu_\Gamma}\right)}. \qquad (11)$$

Here μ_Γ,μ_L and μ_X are the mobilities, and n_Γ,n_L andn_X are the densities of the electrons in the Γ, L and X valleys of the conduction band, respectively.

3. Experimental procedure

3.1. Samples

The barrier-structure samples investigated in the present study were prepared from the same wafers as those used by Bishop *et al.* [4]. The layer structure of the samples is shown in Fig. 1. A 1 μm thick, heavily doped n^+-GaAs contact layer was deposited on the n^+-GaAs substrate. The barrier structure was then grown on this layer in three stages: (i) a 500 Å thick $Ga_{1-y}Al_yAs$ graded barrier, in which the Al concentration (y) increased linearly from 0 to 0.26; (ii) $Ga_{0.74}Al_{0.26}As$ central barrier containing N_w (=0, 2, 4, 7 and 10) n-doped GaAs quantum wells; and (iii) a 500 Å thick $Ga_{1-y}Al_yAs$ graded barrier in which the Al concentration decreased linearly from 0.26 to 0. Finally, a 1μm thick heavily doped n^+-GaAs contact was deposited on the $Ga_{1-y}Al_yAs$ graded barrier. All barrier layers were nominally undoped. The samples were fabricated in the circular mesa geometry of 100 μm diameter.

Table 2. $Ga_{1-y}Al_yAs$ (y=0.26) material parameters used in the calculation of the electron mobility [7, 25].

Longitudinal elastic stiffness constant C_L [10^{11}N/m^2]	1.403
Transverse elastic stiffness constant C_T [10^{11}N/m^2]	0.486
Lattice constant a[Å]	5.6553
High-frequency dielectric constant ε_∞	10.17
Static dielectric constant ε_s	12.35
Piezoelectric constant e_{14} [C/m^2]	-0.177
LO phonon energy $\hbar\omega_{LO}$ [meV]	34.64
Acoustic deformation potential E_A [eV]	8.6
Alloy disorder potential ΔU [eV]	0.30
Electron effective mass (in Γ valley) m^*/m_0	0.089

Structural properties of the barrier-structure samples used in the study are given in Table 1. The doping density in the n^+-GaAs contacts was of the order of 10^{24} m^{-3}, and the doping in the quantum wells was chosen to give a Fermi-level matching that of the contacts, in order to avoid band bending [4, 5]. All barrier structures containing quantum wells in the central barrier were designed to have only one bound state in the well.

3.2. Geometric magnetoresistance measurements

Geometric magnetoresistance (GMR) measurements provide a useful technique to determine the electron mobility in barrier-structure samples of mesa geometry [2, 8, 9, 22–24]. In this technique, a steady magnetic field (B) is applied to the sample parallel to the layers but perpendicular to the vertical current. A dc voltage is applied to the sample, and the vertical current (I) is measured as a func-

Brought to you by | Hacettepe Ueniversitesi
Authenticated
Download Date | 3/12/20 1:58 PM

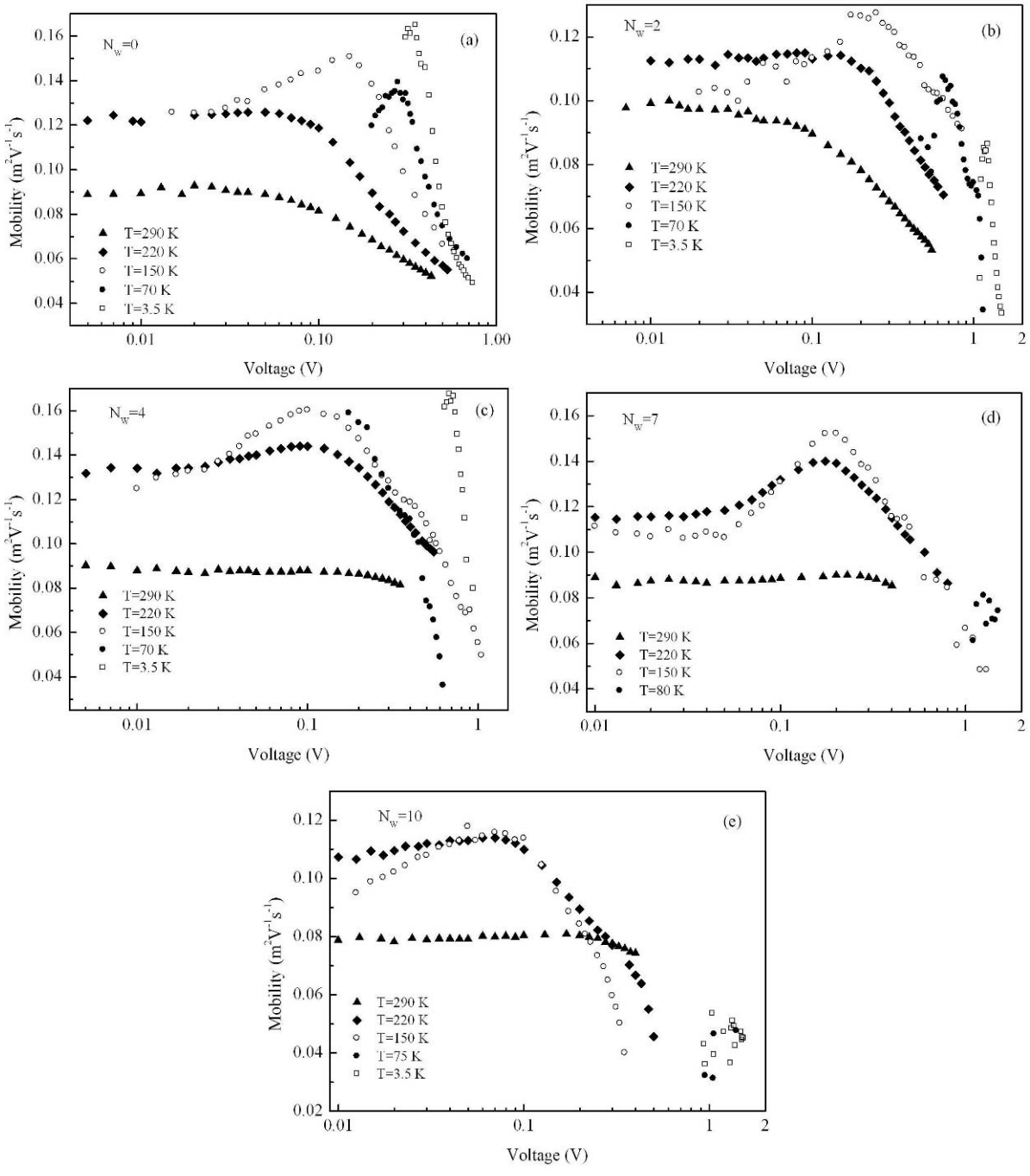

Figure 6. Voltage dependence of the electron mobility measured at selected temperatures for the barrier-structure samples containing (a) N_w=0, (b) 2, (c) 4, (d) 7 and (e) 10 quantum wells.

tion of the magnetic field. The experimental $I-B$ data are then used to obtain the fractional change in magnetoresistance ($\Delta R/R_0$) of the sample as a function of the magnetic field. The magnetic field dependence of $\Delta R/R_0$ is given by

$$\frac{\Delta R}{R_0} = \frac{R(B)-R_0}{R_0} \cong (\mu_{GMR}B)^2 \text{ for } (\mu_{GMR}B)^2 \ll 1, \quad (12)$$

where R_0 is the resistance at zero magnetic field, $R(B)$

Brought to you by | Hacettepe Ueniversitesi
Authenticated
Download Date | 3/12/20 1:58 PM

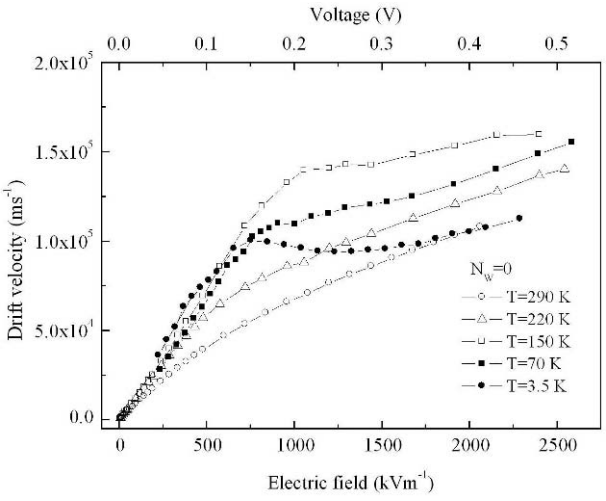

Figure 7. Electric-field dependence of the electron drift velocity in the barrier-structure sample without quantum wells (N_w=0) determined at the temperatures quoted.

is the magnetoresistance, and μ_{GMR} is the GMR mobility, which is usually taken approximately equal to the Hall mobility [2, 4, 8, 9, 22–24]. In order to use the GMR technique, the magnetic field must be low enough to ensure that $(\mu_{GMR}B)^2 \ll 1$, and the mesa diameter (d_m) must be much greater than the total thickness (L) of the barrier layers [4, 8, 23]. For the samples used in the present study $L \cong 0.2$ μm (see Table 1) and d_m=100 μm, the highest measured value of the mobility is $\cong 0.17$ $m^2V^{-1}s^{-1}$, and the magnetic field is in the range 0.2-2.2 T. Therefore, both conditions are fulfilled in our experiments.

The GMR measurements were carried out in the dark as functions of temperature from 80 to 290 K at low applied voltages (0.01-0.1 V), and applied voltage (0.005-1.6 V) at selected temperatures in the range 3.5-290 K. The measurements were performed in a three-stage, closed-cycle refrigeration system (HS-4 Heliplex, APD Cryogenics) using a source/measure unit (Keithley 236).

4. Results and discussion

Typical examples for the variation of fractional magnetoresistance ($\Delta R/R_0$) with magnetic field are shown in Figs. 2a and 2b. The $\Delta R/R_0$ increases linearly with B^2. The electron mobility (μ_{GMR}) was determined by fitting Eq. (12) to the experimental $\Delta R/R_0$ versus B curves measured for each temperature and each applied voltage. In this procedure μ_{GMR} was taken as an adjustable parameter, which was assumed to be independent of the magnetic field.

4.1. Temperature dependence of the electron mobility

To determine the temperature dependence of the electron mobility in the barrier-structure samples, GMR measurements were carried out in the temperature range 80-290 K at low applied voltages between 0.01 and 0.1V. In this set of measurements, the applied voltage was low enough to permit the assumption that the electrons be in thermal equilibrium with the lattice. Since the graded barriers limit the tunnelling current at low applied voltages, it was not possible to determine the low-field electron mobility at temperatures below 80 K.

Examples for the variation of electron mobility with temperature are presented in Figs. 3a to 3e. At the lowest voltage (0.01 V), the mobility rises with increasing temperature, passes through a broad maximum at a temperature $T_m \approx 200$ K, and decreases at higher temperatures. This behaviour is more clearly demonstrated by the $\mu_{GMR}(T)$ curves obtained for the samples containing N_w=4, 7 and 10 quantum wells. The $\mu_{GMR}(T)$ curves determined at 0.05 and 0.1V exhibit similar features, however, the mobility reaches the maximum at lower temperatures. As the applied voltage is increased from 0.01 to 0.1 V, the electron mobility measured at temperatures below T_m increases for all the samples, except the one with N_w=10 quantum wells.

The temperature dependence of the Hall mobility in bulk $Ga_{1-y}Al_yAs$ alloys has been investigated in several studies [7, 11–13, 19]. The mobility has been reported to increase with increasing temperature from 100 K, reach a broad maximum at about 200 K, and decrease at higher temperatures. The increase of mobility as the temperature is increased from 100 to 200 K has been attributed to ionized impurity scattering. The decrease of mobility at temperatures above 200 K has been explained by polar optical phonon scattering. However, for bulk $Ga_{1-y}Al_yAs$ samples, in which space-charge scattering is significant, the reduction of electron mobility with temperature above 200 K has been attributed to the combined effect of polar optical phonon scattering and space-charge scattering [7, 11–13, 18].

In the light of these earlier studies, for the barrier-structure samples containing N_w=4, 7 and 10 quantum wells in the central barrier, the increase of electron mobility as the temperature is increased from 80 to about 200 K can be ascribed to ionized impurity scattering (see also [5]). However, at temperatures below 200 K, the slope of the $\mu_{GMR}(T)$ curves measured at 0.01 V for the samples with N_w=0 and 2 is relatively small (Figs. 3a and 3b), indicating that space-charge scattering is in effect in these samples.

The $\mu_{GMR}(T)$ curves obtained at 0.01 V for the barrier-

Brought to you by | Hacettepe Ueniversitesi
Authenticated
Download Date | 3/12/20 1:58 PM

structure samples with different numbers (N_w) of quantum wells in the central barrier are compared in Fig. 4. The figure demonstrates that the maximum mobility measured at $T_m \approx 200$ K decreases significantly as N_w increases from 4 to 10 (that is, as the barrier width L_B between the quantum wells decreases from 310 to 77 Å). Electrons encountering a quantum well would undergo reflection from well-barrier interfaces, so their mobility would decrease [4, 5]. The influence of this quantum-well scattering on the electron mobility is expected to be more pronounced for the barrier structures in which the barrier width L_B is smaller [5, 9]. The $\mu_{GMR}(T_m)$ data measured in the present study, for the barrier-structure samples with N_w=4, 7 and 10, are in line with these theoretical predictions. However, the $\mu_{GMR}(T_m)$ values determined for the samples with N_w=0 and 2 are markedly smaller than that for the sample with N_w=4. This experimental finding indicates that space-charge scattering is important in the determination of the electron mobility in the samples with N_w=0 and 2, and growing 2 quantum wells (one at each end of a wide central barrier) is not adequate to prevent the formation of space charge in the barrier layer between the wells.

4.2. Analysis of the scattering mechanisms that determine the temperature dependence of electron mobility

To carry out a detailed analysis of the scattering mechanisms that limit the mobility of electrons in GaAs/$Ga_{1-y}Al_yAs$ barrier structures, the mobility μ_i determined by each intra-valley scattering mechanism was calculated as a function of temperature from 80 to 300 K by using the Equations given in section 2. The material parameters used in the calculation of the mobilities μ_A, μ_{DP}, μ_{PE}, μ_{ii}, μ_{SC} and μ_{PO} are given in Table 2. The space-charge scattering mobility μ_{SC} was calculated only for the samples with N_w=0 and 2, because the space-charge effect was not observed [4, 26] in the current-temperature characteristics of the samples with N_w=4, 7 and 10. Because the lattice mismatch between the GaAs and $Ga_{1-y}Al_yAs$ layers is very small [25], the effect of dislocation scattering due to lattice mismatch [27] on the electron mobility in the barrier-structure samples was not considered in the present study. Intervalley scattering was assumed to be negligible at low applied voltage, because almost all electrons reside in the Γ valley of the conduction band [13]. The current-temperature characteristics of the samples with N_w=4, 7 and 10 did not exhibit any evidence for miniband conduction. This could be due to the fact that the width of the first subband was much smaller than the collision broadening, as determined from the mobility measurements at low applied voltage. For instance, for the sample with N_w=10, the width of the first subband is 4.5 meV and the collision broadening is about 15 meV. Therefore, the influence of subband width on the vertical transport in these samples was not taken into account.

In order to calculate the mobility μ_{ii} determined by ionized impurity scattering, the donor (N_D) and acceptor (N_A) densities are required (see Eqs. (1) and (2)). Acceptor impurities were introduced by unintentional doping during the growth of the barrier structures [2, 4]. The acceptor densities N_A in the samples with N_w=0 and 2 were assumed to be equal to the space-charge densities N_S=4.0×10^{21} m^{-3} and 4.1×10^{21} m^{-3}, respectively, as determined from the current-temperature measurements at low voltage (0.01 V) [26]. Then, the mobility μ_{GMR} measured at 140 K for each of these samples was fitted to the total mobility μ_{tot} calculated at the same temperature from Eq. (1), by taking the N_SA product (in Eq. (9)) as a fitting parameter and neglecting N_D in Eq. (2). The N_SA values that provide the best fit between the experimental mobility and the calculated total mobility are 7.2×10^7 m^{-1} and 7.1×10^7 m^{-1} for the samples with N_w=0 and 2, respectively. These N_SA values are comparable to the data 3×10^7, 1.7×10^7 and 2×10^7 m^{-1} reported in the literature for bulk $Ga_{0.75}Al_{0.25}As$ [13], $Ga_{0.68}Al_{0.32}As$ [18], and $Ga_{0.65}Al_{0.35}As$ [11], respectively. The donor density N_D in the samples with N_w=4, 7 and 10 was estimated to be about 4×10^{23}m^{-3} (which is slightly smaller than the doping level of the quantum wells in the central barrier [4]), under the assumption that ionized impurity scattering is dominant at low temperatures. More specifically, the N_D value for each of latter samples was deduced by matching the mobility μ_{GMR} measured at 110 K to the ionized impurity scattering mobility μ_{ii} calculated at that temperature. In this procedure N_A was neglected, because the space-charge effect was not observed in these samples.

Examples for the comparison between the calculated $\mu_i(T)$ and $\mu_{tot}(T)$ curves and the experimental $\mu_{GMR}(T)$ data measured at 0.01 V are presented in Figs. 5a and 5b for the samples with N_w=0 and 10, respectively. For all the barrier-structure samples investigated, the calculated mobilities μ_A, μ_{DP} and μ_{PE} are about two orders of magnitude larger than the measured mobility. This suggests that the effects of alloy-disorder scattering and acoustic phonon scattering on the mobility of electrons in vertical transport are negligibly small at all temperatures. The results show that space-charge scattering is dominant in the samples with N_w=0 and 2 at all temperatures, while the effect of ionized impurity scattering on the mobility is negligible (Fig. 5a). In the samples containing N_w=4, 7 and 10 quantum wells, the mobility is primarily limited by ionized impurity scattering (Fig. 5b). The effect of

Brought to you by | Hacettepe Ueniversitesi
Authenticated
Download Date | 3/12/20 1:58 PM

polar optical phonon scattering increases progressively at temperatures above 200 K, leading to a decrease in the mobility, as observed in all the samples studied (see Fig. 3).

For the samples containing N_w=4, 7 and 10 quantum wells, the electron mobility measured at temperatures above about 200 K is somewhat smaller than the calculated total mobility (see Fig. 5b). This suggests that additional scattering mechanisms, which are not considered in the calculation of $\mu_{tot}(T)$, come into effect in the determination of the electron mobility in these samples. As the number (N_w) of quantum wells increases, the reflection of electrons from the well-barrier interfaces increases, thereby leading to a decrease in the measured mobility of electrons in vertical transport [5, 9]. It is well established that the mobility of two-dimensional electrons in parallel transport in GaAs/$Ga_{1-y}Al_yAs$ ($y \cong 0.3$) multiple quantum wells (MQWs) is primarily limited by interface roughness (IFR) scattering [28, 29]. IFR scattering would also influence the vertical mobility of electrons in the barrier-structure samples containing N_w (=4, 7 and 10) quantum wells [30, 31]. Dharssi and Butcher [30] calculated the IFR scattering-limited mobility in the growth direction at 300 K for a low-density, non-degenerate electron gas in short-period GaAs/$Ga_{0.7}Al_{0.3}As$ superlattices. They found that the mobility limited by IFR scattering is up to an order of magnitude less than the predicted LO phonon scattering-limited mobility. Therefore, the difference between the measured mobility (μ_{GMR}) and the calculated total mobility (μ_{tot}) observed above about 200 K for the barrier-structure samples with N_w=4, 7 and 10 can be attributed, at least in part, to the quantum-mechanical reflection due to the quantum wells and to IFR scattering. Nevertheless, further theoretical work is required to calculate the effects of IFR scattering on the vertical mobility in barrier structures containing MQWs, in which the electrons are strongly localised in the first subband.

4.3. Variation of electron mobility with applied voltage

Examples for the variation of electron mobility with applied voltage, measured at selected temperatures in the range 3.5-290 K, are shown in Figs. 6a to 6e. The $\mu_{GMR}(V)$ curves obtained at 3.5, 70 and 150 K for the samples with N_w=0, 2 and 4 demonstrate that the mobility increases slightly with increasing voltage, passes through a maximum, and decreases rapidly with further rise in the voltage. For the samples with N_w=0 and 2, the mobility measured at 220 and 290 K remains essentially constant up to ~0.06 V and decreases at higher voltages. The $\mu_{GMR}(V)$ curves measured at 150 and 220 K for the samples containing N_w=7 and 10 quantum wells exhibit similar behaviour. The mobility measured at 290 K for the samples with N_w=4, 7 and 10 is practically independent of the applied voltage up to ~0.25 V and tends to decrease at higher voltages.

The voltage V_m at which the mobility becomes maximum is found to be a function of the temperature. For the samples with N_w=0, 2 and 4, V_m decreases substantially when the temperature is increased from 3.5 to 220 K (Figs. 6a, 6b and 6c). In the low-voltage region ($V_S < V_m$), the increase of mobility with applied voltage can be attributed to ionized impurity scattering [32]. The reduction of electron mobility at high voltages ($V_S > V_m$) is likely to be due to intervalley scattering of hot electrons from the Γ valley into the L (and X) valleys in the conduction band, where they will have lower mobilities. The GMR measures an average of the mobilities of the three electron populations (see Eq. (11)). In the case of bulk GaAs and $Ga_{1-y}Al_yAs$ ($y \leq 0.35$) alloys [18, 32] and GaAs/$Ga_{1-y}Al_yAs$ barrier structures with rectangular potential barrier containing MQWs [9], the mobility reduction in the high-voltage region has been explained by intervalley scattering of hot electrons. A similar interpretation should also be valid for the barrier-structure samples investigated in the present study.

When the voltage (electric field) applied to the barrier-structure sample exceeds a given threshold, hot electrons scatter from the Γ valley to the L (and X) valleys, which are at higher energies and have larger electron effective mass but smaller mobility. The duration times of electrons in the L (and X) valleys were found to be about an order of magnitude longer than the scattering time back to the Γ valley [9, 32, 33]. Earlier studies [18, 34, 35] found that the mobilities μ_Γ, μ_L and μ_X in bulk GaAs and $Ga_{1-y}Al_yAs$ ($y < 0.32$) alloys fall in the ranges 0.2-0.3, 0.03-0.05 and 0.03-0.04 $m^2V^{-1}s^{-1}$, respectively. In addition, the ratio μ_Γ:μ_L was found to be about 8:1 (Refs. [13, 34]). Hence, one would expect the Hall mobility estimated from Eq. (11) to be much smaller than the mobility μ_{GMR} measured at low applied voltage ($V_S \ll V_m$). However, since the carrier densities in the Γ, L and X valleys are not known, it is not possible to determine separately the mobilities μ_Γ, μ_L and μ_X for the barrier-structure samples used in the present study. For the sample with N_w=7, the mobility (μ_{GMR}) values measured at 80 K and at high voltages (1.1-1.5 V) fall in the range 0.05-0.08 $m^2V^{-1}s^{-1}$ (Fig. 6d). Similarly, for the sample with N_w=10, the μ_{GMR} values measured at 3.5 and 75 K and at high voltages (0.95-1.5 V) fall in the range 0.03-0.05 $m^2V^{-1}s^{-1}$ (Fig. 6e). These mobility values, determined for the barrier-structure samples investigated in this study, are comparable to those reported [18, 34, 35] for μ_L and μ_X of electrons in the L

Brought to you by | Hacettepe Ueniversitesi
Authenticated
Download Date | 3/12/20 1:58 PM

and X valleys of bulk GaAs and $Ga_{1-y}Al_yAs$ (y <0.32) alloys. The results suggest that, when a voltage higher than about 1.0 V is applied (at low temperatures) to the barrier-structure samples containing N_w=7 and 10 quantum wells, an important proportion of electrons are transferred from the Γ valley to the L and X valleys.

Finally, we deduced the electron drift velocity V_d as a function of applied electric field from the experimental $\mu_{GMR}(V)$ data. As a first approximation, the drift velocity was calculated from $V_d = \mu F$ by taking $\mu = \mu_{GMR}$ and $F = V_S/L$ (the average applied electric field). Examples for the $V_d(F)$ curves obtained for the sample with N_w=0 are shown in Fig. 7. Initially, the drift velocity increases linearly with electric field; after the electric field exceeds a certain value the drift velocity continues to increase, but with a progressively decreasing slope. The sublinear deviation of the experimental $V_d(F)$ curve at high electric fields is due to the heating of electrons. The $V_d(F)$ curves obtained for the barrier-structure samples investigated in this study show similar features with those calculated using Monte Carlo methods [36–39], and those measured at 300 K for bulk $Ga_{1-y}Al_yAs$ (y <0.45) alloys [13], and at 15 K for GaAs/$Ga_{1-y}Al_yAs$ barrier structures containing MQWs [9].

When the excess kinetic energy of hot electrons in the Γ valley of bulk GaAs reaches the intravalley LO phonon energy, the hot electrons cool down by emitting LO phonons; consequently, the slope of the $V_d(F)$ curve decreases. When the energy-input rate of electrons becomes equal to the energy-loss rate to the lattice, the drift velocity is expected to reach a maximum (saturation) value and to decrease at higher electric fields, due to intervalley scattering (see for instance [32]). The decrease in electron drift velocity with electric field is known as negative differential resistance (NDR), which is seen clearly on the $V_d(F)$ curve obtained at 3.5 K (Fig. 7). However, since the intervalley energy separations $\Delta E_{\Gamma L}$ and $\Delta E_{\Gamma X}$ in bulk $Ga_{1-y}Al_yAs$ (y ≤0.26) alloys are smaller than the corresponding energy differences in GaAs [13, 33, 35], the $V_d(F)$ curves obtained for the barrier-structure samples at temperatures above 70 K did not clearly exhibit NDR behavior.

5. Conclusions

The geometric magnetoresistance technique was used to measure the mobility of electrons in the vertical transport in GaAs/$Ga_{1-y}Al_yAs$ (y ≤0.26) barrier-structure samples containing N_w (=0, 2, 4, 7 and 10) quantum wells in the central barrier. The results show that space-charge scattering is dominant in the samples with N_w=0 and 2, at all temperatures, while ionized impurity scattering is dominant in the samples containing N_w=4, 7 and 10 quantum wells. Polar optical phonon scattering becomes significant in all the samples at high temperatures, leading to a decrease of mobility at temperatures above 200 K. The effects of alloy disorder, acoustic deformation potential and acoustic piezoelectric scattering mechanisms on the mobility are negligibly small. The difference between the measured mobility and the calculated total mobility for the samples with N_w=4, 7 and 10, observed above 200 K, is attributed to the reflection of electrons from well-barrier interfaces in the quantum wells and to interface roughness scattering.

The mobility-temperature curves measured at low voltage exhibit a broad maximum at about 200 K. The maximum mobility decreases systematically as the number of quantum wells in the central barrier increases from N_w=4 to 10. This experimental finding is in line with the theoretical prediction [5] that the electrons will scatter more frequently from the well-barrier interfaces with increasing N_w, and their mobility will decrease as a consequence. However, the maximum mobility data for the samples with N_w=0 and 2, in which space-charge scattering is dominant, do not follow this trend.

The mobility of electrons in vertical transport increases slightly as the applied voltage is increased, passes through a maximum, and decreases rapidly with further increase in the voltage. The decrease of electron mobility at high voltages is explained by intervalley scattering of hot electrons. This suggests that optimisation of devices which incorporate barrier structures should consider the properties of the L and X valleys as well.

Acknowledgments

We would like to thank Professor Naci Balkan (at Essex University, UK) for providing the samples and Dr. Ceyhun Bulutay (at Bilkent University) for valuable discussions. We are grateful to TÜBITAK Ankara (project No: TBAG-2218, 102T111) for financial support.

References

[1] B.F. Levine, J. Appl. Phys. 74, R1 (1993)
[2] M.E. Daniels et al., J. Appl. Phys. 74, 5606 (1993)
[3] M.E. Daniels et al., Semicond. Sci. Technol. 9, 595 (1994)
[4] P.J. Bishop, M.E. Daniels, B. K. Ridley, J. S. Roberts, G. Hill, Semicond. Sci. Technol. 11, 873 (1996)

Brought to you by | Hacettepe Ueniversitesi
Authenticated
Download Date | 3/12/20 1:58 PM

[5] M.E. Daniels, P.J. Bishop, B.K. Ridley, Semicond. Sci. Technol. 12, 375 (1997)
[6] P.J. Bishop, M.E. Daniels, B.K. Ridley, Semicond. Sci. Technol. 13, 482 (1998)
[7] A.K. Saxena, Phys. Rev. B 24, 3295 (1981)
[8] D.C. Look, Electrical Characterization of GaAs Materials and Devices (John Wiley & Sons, New York, 1989)
[9] A. Fraenkel, E. Finkman, S. Maimon, G. Bahir, J. Appl. Phys. 75, 3536 (1994)
[10] L.M. Falicov, M. Cuevas, Phys. Rev. 164, 1025 (1967)
[11] G.B. Stringfellow, J. Appl. Phys. 50, 4178 (1979)
[12] G.B. Stringfellow, H. Künzel, J. Appl. Phys. 51, 3254 (1980)
[13] P.K. Bhattacharya, U. Das, M.J. Ludowise, Phys. Rev. B 29, 6623 (1984)
[14] F. Bosc, J. Sicart, J.L. Robert, Semicond. Sci. Technol. 14, 64 (1999)
[15] C.M. Wolfe, G.E. Stillman, W.T. Lindley, J. Appl. Phys. 41, 3088 (1970)
[16] A. Fortini, D. Diguet, J. Lugand, J. Appl. Phys. 41, 3121 (1970)
[17] L.R. Weisberg, J. Appl. Phys. 33, 1817 (1962)
[18] A.K. Saxena, K.S. Gurumurthy, J. Phys. Chem. Solids 43, 801 (1982)
[19] K. Kaneko, M. Ayabe, N. Watanebe, Inst. Phys. Conf. Ser. 33a, 216 (1977)
[20] J.R. Hauser, M.A. Littlejohn, T.H. Glisson, Appl. Phys. Lett. 28, 458 (1976)
[21] B.K. Ridley, In: J. Shah (Ed.), Hot Carriers in Semiconductor Nanostructures: Physics and Applications (Academic Press, New York, 1992) 17.
[22] T.R. Jervis, E. F. Johnson, Solid State Electronics 13, 181 (1970)
[23] J.W. Orton, J. Phys. D Appl. Phys. 6, 851 (1973)
[24] M.J. Kane et al., J. Appl. Phys. 73, 7966 (1993)
[25] S. Adachi, J. Appl. Phys. 58, R1 (1985)
[26] H. Çelik, M. Cankurtaran, S. Altunöz, N. Balkan, Investigation of vertical transport in GaAs/$Ga_{1-y}Al_yAs$ barrier structures containing multiple quantum wells, Final Report to project: TÜBITAK TBAG-2218, Ankara, 2006 (in Turkish).
[27] R. Jazsek, J. Mater. Sci. 12, 1 (2001)
[28] H. Çelik, M. Cankurtaran, A. Bayrakli, E. Tiras, N. Balkan, Semicond. Sci. Technol. 12, 389 (1997)
[29] N. Balkan et al., Superlattices and Microstructures 22, 263 (1997)
[30] I. Dharssi, P.N. Butcher, J. Phys.-Condens. Mat. 2, 4629 (1990)
[31] G. Etemadi, J.F. Palmier, Solid State Commun. 86, 739 (1993)
[32] P.Y. Yu, M. Cardona, Fundamentals of Semiconductors: Physics and Materials Properties (Springer-Verlag, Berlin, 1995)
[33] C.L. Collins, P.Y. Yu, Phys. Rev. B 30, 4501 (1984)
[34] D.E. Aspnes, Phys. Rev. B 14, 5331 (1976)
[35] A.K. Saxena, Phys. Rev. B 25, 5428 (1982)
[36] K.F. Brennan, D.H. Park, K. Hess, M.A. Littlejohn, J. Appl. Phys. 63, 5004 (1988)
[37] V.M. Fichetti, IEEE T. Electron. Dev. 38, 634 (1991)
[38] X. Zhou, H.S. Tan, Int. J. Electronics 76, 1049 (1994)
[39] O.O. Cellek, S. Memis, U. Bostanci, S. Ozer, C. Besikci, Physica E 24, 318 (2004)

Brought to you by | Hacettepe Ueniversitesi
Authenticated
Download Date | 3/12/20 1:58 PM